Jordan Journal of Civil Engineering, Volume **3**, No. **1**, **2009**

Time Dependent Capacity Increase for Driven Pile in Cohesionless Soil

Ahmed S. Alawneh [1)]***, Osama K. Nusier*** [2)] ***and Murad S. Awamleh***[3)]

[1)] Professor of Civil Engineering, Civil Engineering Department, Jordan University of Science and Technology
[2)] Associate Professor of Civil Engineering, Civil Engineering Department, Jordan University of Science and Technology, Irbid 22110 – Jordan, e-mail: nosama@just.edu.jo
[3)] Former Graduate Student

ABSTRACT

The increase in driven pile capacity with time is termed set-up. The mechanism contributing to this phenomenon is not yet fully understood. Moreover, a rational approach to account for the increase in driven pile capacity with time in design has not yet been developed. In this study, a database comprising of 55 pile load tests (static and dynamic tests) were collected from the current engineering literature. The piles were driven in cohesionless soils with sand relative density varying from loose to dense. The measured capacities of the database piles with time were correlated to pile characteristics and soil properties. Pile set-up was found to be a phenomenon related to an increase in pile shaft friction with time and increases with decreasing pile diameter. On the other hand, pile set-up was found to increase with increasing pile penetration depth and thus with pile slenderness ratio.

A new approach for the estimation of pile set-up in cohesionless soils is presented in this study. The new approach considers the effects of pile characteristics and soil properties. Comparison of predicted and measured pile set-up using the developed method in this study indicates reasonable agreement. Also, comparison of prediction using the new approach with those made using previously published methods indicates that the developed method in this study yields better results.

KEYWORDS: Time dependent capacity, Set-up, Cohesionless soil, Pile, Capacity increase.

INTRODUCTION

Many types of structures such as multi-storey buildings, bridges, parking garages and stadiums are supported on deep foundation consisting of driven piles. Deep foundation cost, relative to the structure cost, ranges typically from 5% for some buildings to as much as 30% for some bridges (Bullock and Schmertmann, 2003). To meet the best economical design, quality control and assurance, engineers routinely test the capacity of deep foundation during and after installation using both static and dynamic methods. For driven piles, these tests often indicate changes (increases) in capacity with time after installation. During pile driving, excess pore water pressures in the surrounding soil is generated. Dissipation of the excess pore water pressures leads to an increase in pile capacity with time.

In cohesive and cohesionless soils, it was observed that pile capacity continues to increase with time after complete dissipation of excess pore water pressure. The increase in pile capacity over time that takes place after the dissipation of excess pore water pressure induced from pile driving is termed soil /pile set-up which is primarily associated with an increase in shaft capacity

Accepted for Publication on 15/1/2009.

(Axelsson, 2000).

The common belief that pile set-up in cohesionless soils is primarily due to the dissipation of excess pore water pressure is not correct. The time for complete dissipation of pore pressure was observed by Plantema (1948) to be 5 minutes for coarse sand and 45 minutes for silty sand, indicating that the dissipation of excess pore water pressure can't explain the observed large increase in bearing capacity that takes place in cohesionless soils over several months or even years.

The mechanisms contributing to set-up especially for driven piles in cohesionless soils are not clearly understood. Schmertmann (1991) and Chow et al. (1997) presented hypotheses which state that long-term set–up for driven piles in cohesionless soils can be divided into:

(1) Stress relaxation (creep) in the surrounding soil arch, which leads to an increase in horizontal effective stress on the shaft.
(2) Soil aging, which leads to an increase in stiffness and dilatancy of the soil.

Both mechanisms start directly after pile installation. However, it is unclear which one of these mechanisms is predominant under dissimilar conditions, and also how long this process continues.

The main objectives of this research is to develop a semi–empirical relationship to predict long- term pile capacity increase over time using short-term pile capacity data, pile characteristics and soil properties. This is very important because if the increase in pile capacity over time is accounted for properly in design, foundation cost (length, diameter and driving energy) will be reduced. To satisfy this objective, a review of the current literature is made and all well-documented field case histories of pile set–up in cohesionless soils are collected. These field cases form the data base for this study.

Short-Term Set-Up

For most cohesionless soils, short-term set-up is defined as the increase in capacity that takes place within 24 hours, during which nearly all the excess pore pressure is expected to dissipate. However, for most sands, short-term set-up due to the dissipation of excess pore pressure normally takes place within a few minutes, or at most a few hours. Furthermore, part of the short-term set-up will, to some extent, be influenced by the same mechanism involved during long-term set-up (Axelsson, 2000).

Axelsson (2000) presented two case histories of short-term set-up. The first case was reported by Sevilla et al. (1998) where piles driven into glacial till were tested over time up to 15 days after the End Of Initial Driving (EOID). Sevilla et al. (1998) observed that the measured set-up which was in the range of 32-80% took place within the first 48 hours. This may indicate that in the absence of any long-term effects, the pore pressure dissipation is the main cause behind the increase in pile capacity with time. The second case history was reported by Castelli and Hussein (1998) where driven piles installed into fine sand with interbedded very stiff clay were tested over time up to 20 days after the End Of Initial Driving (EOID). Castelli and Hussein (1998) concluded that the observed set-up which took place within 24 hours was primarily due to the dissipation of excess pore water pressure.

Long-Term Set-Up

Long-term set-up is defined as an increase in pile capacity over time that takes place after the dissipation of excess pore pressures induced by pile driving. The first well-documented case of long term set-up in cohesionless soils was reported by Tavenas and Audy (1972). Tavenas and Audy (1972) conducted a static pile load test (compression) on 45 precast concrete piles driven into a medium dense deposit of medium to fine sand. The results indicated that during the first 15-20 days the measured pile capacity reached an average value of about 70% higher than the observed capacity for a reference pile tested 12 hour after driving. Tavenas and Audy (1972) concluded that the increase in pile capacity with time must be related to changes occurring in the sand structure around the pile and not to the dissipation of excess pore pressure.

Fellenius (1989) tested the capacity of a driven pile in cohesionless soils over time and found that pile set-up occurred rapidly during the first day after initial pile

driving and then continued to increase but at slow rate for at least several weeks. 50 percent increase in pile capacity was observed by Fellenius (1989) in 20 days after pile driving.

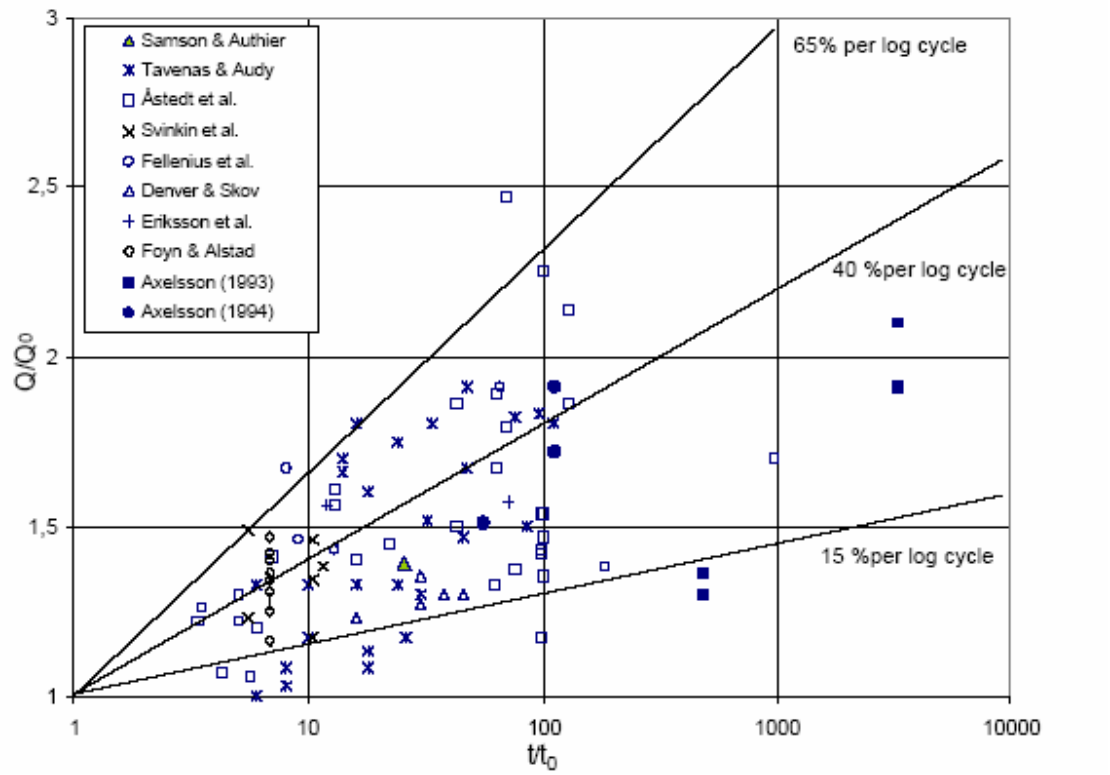

Figure (1): Case histories of long-term pile set-up where t_o is between 0.5 - 4 days after (EOD), (Axelsson 2000).

Chow et al. (1998) studied data collected from 11 studies on driven piles in sand with long-term set-up effects. A long-term pile set-up in the range of 50% to 150% over 100 days was observed in the collected data. Chow et al. (1998) also performed static pile load test on open and closed- ended driven piles in dense marine sand. Chow et al. (1998) observed 85% increases in shaft capacity between six months and five years after pile driving. Chow et al. (1998) suggested that the main reason beyond this phenomenon is the development of a circumferential arching mechanism during pile driving that limits the radial stress acting on the pile shaft and the creep of the surrounding soil leads to a break down of these arching stresses, allowing an increase in radial stress and hence a gain in pile shaft capacity.

York et al. (1994) reported that displacement piles driven in cohesionless soil show time-dependent increase in axial capacity in the range of 40-80% as determined by loading tests. York et al. (1994) stated that set-up results from a loss of strength due to disruption of the structure of the surrounding sand during pile driving followed by a recovery in strength as the soil structure heal at a constant effective stress.

Svinken (1996) studied the capacity of driven piles as a function of time. The piles were driven in dense silty sand, and it was observed that set-up gradually increased during the first 10 days after the End Of Initial Driving (EOID) with various rates for different piles, after that a stabilization of set-up was observed. Long et al. (1999) compiled a database of set-up cases for driven piles in

clayey soil, mixed soil and sandy soil. The sandy soil group consists of six case histories (mainly the same ones as in (Chow et al., 1998). A lower bound of 20 % and an upper bound of 100 % increase in pile capacity per log cycle of time were suggested in sandy soil, but only for the first 100 days after driving. Long et al. (1999) determined that although the largest set-up occurred in the first 10 days after driving, set-up appeared to continue for up to 500 days.

Axelsson (2000) stated that the reference pile capacity in the data base collected by chow et al. (1998) and long et al. (1999) was measured at the End Of Initial Pile Driving (EOID). Hence, part of the presented set-up would be due to pore pressure effect. In order to avoid this situation, Axelsson (2000) compiled a database of case histories on friction piles, where the reference pile capacity was measured between 12 hours and 4 days after EOID, during this period of time complete pore pressure dissipation can be expected to take place in sandy soil. The database consists of 181 loading tests performed on 71 piles at 16 sites. Total capacity has been used in this study and a logarithm of time versus pile capacity ratio was plotted as shown in Figure (1). In Figure (1) two lines representing 15% (lower bound) and 65% (upper bound) increase in pile capacity per log cycle of time are shown. The data shown in Figure (1) clearly indicate that pile set-up can continue for several months after the end of pile driving.

Estimation of Pile Set-Up (Previous Studies)

Skov and Denver (1988) proposed a method to estimate the long-term pile capacity *(Q_t)* in cohesive and cohesionless soils from the short-term pile capacity (Q_o) using the following correlation:

$$Q_t = Q_o\left[1 + A\log(\frac{t}{t_o})\right] \quad (1)$$

where

t = Time after the end of initial driving.

t_o = Initial reference time elapsed since end of driving = 0.5 day.

Q_o= Pile capacity at time (t_o).

Q_t = Pile capacity at time (t).

Skov and Denver (1988) recommended using A = 0.2 for piles in cohesionless soils. Long et al. (1999) indicates that (A) may vary from 0.2 to 0.1. Chow et al. (1998) reported that, based on data collected from the work of 14 researchers, values of (A) vary from 0.25 to 0.75. Axelsson (1998) reported (A) values from 0.2 to 0.8.

Despite that equation (1) was developed by Skov and Denver (1988) based on limited case histories in cohesionless soils, it remains the most commonly used method to estimate the increase in pile capacity with time by the current practitioners. Case histories presented by Tavenas and Audy (1972), Fellenius et al. (1989) and York et al. (1994) confirm equation (1), at least up to a month from the end of pile driving.

On the other hand, Svinkin (1996) developed the following equation based on load test data on five concrete piles in dense silty sand:

$$Q_t = (1.025 \text{ to } 1.4)\, Q_o\, t^{0.1} \quad (2)$$

This equation was developed for a specific data set, and seems to underpredict long-term pile capacity for most other published case histories. Moreover, the maximum time for all the tests used in developing equation (2) is less than 25 days. Accordingly, it can be concluded that equation (2) is applicable just for a maximum time of 25 days after pile driving.

Tan et al. (2004) suggested that long-term pile capacity increase in cohesionless soil can be predicted with reasonable accuracy based on short-term results by modifying the equation which was proposed by Bogard and Matlock (1990) using hyperbolic formulation:

$$\frac{Q_{t2}}{Q_{t1}} = \frac{(0.2T_{50}+t_2)(T_{50}+t_1)}{(0.2T_{50}+t_1)(T_{50}+t_2)} \quad (3)$$

where:

t_1 and t_2 = time in days after the end of initial driving.

Q_{t1} and Q_{t2} = pile capacity at t_1 and t_2.

T_{50} = time required to release 50% of pile set-up.

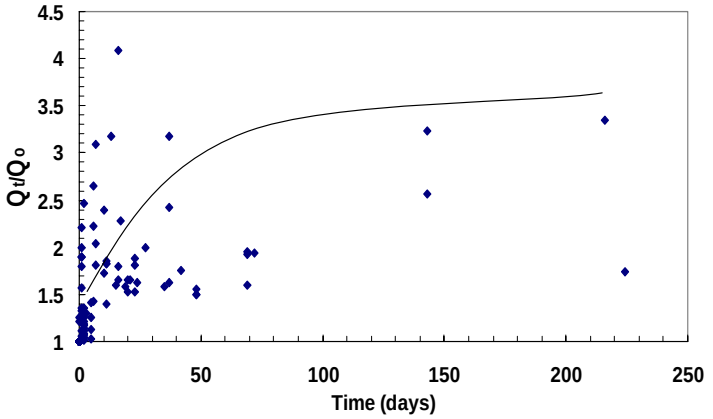

Figure (2-a): A plot of Q_t/Q_o versus time.

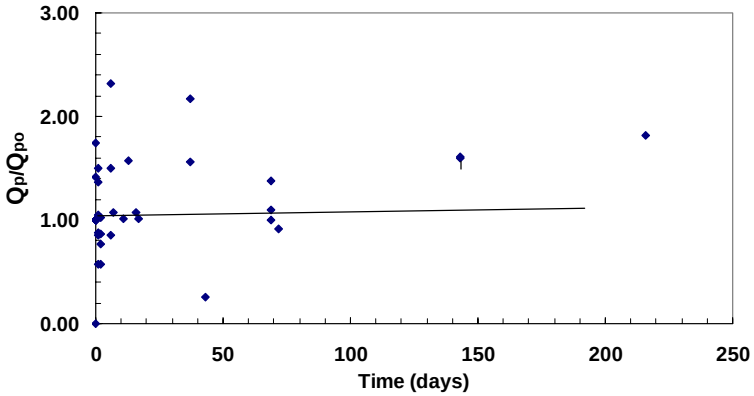

Figure (2-b): A plot of Q_p/Q_{po} versus time.

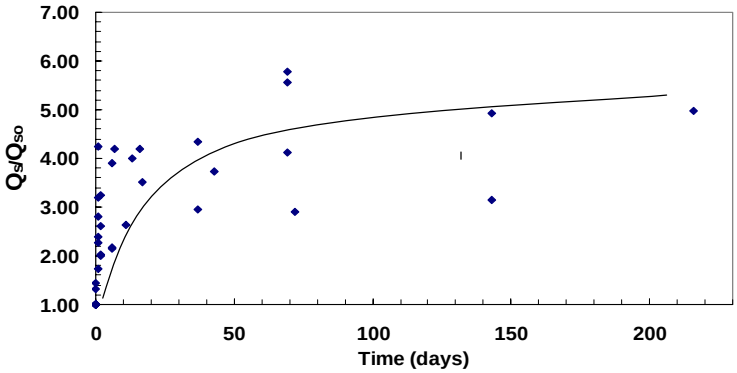

Figure (2-c): A plot of Q_s/Q_{so} versus time.

Figure (2): Total, point and shaft capacity versus time for the data base in the study.

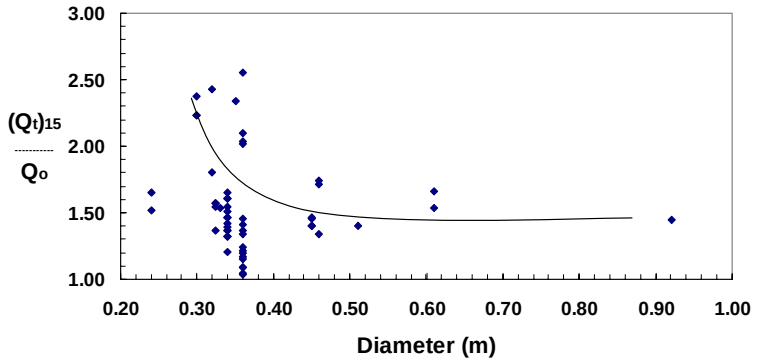

Figure (3-a): A Plot of $\frac{(Q_t)_{15}}{Q_o}$ versus pile diameter.

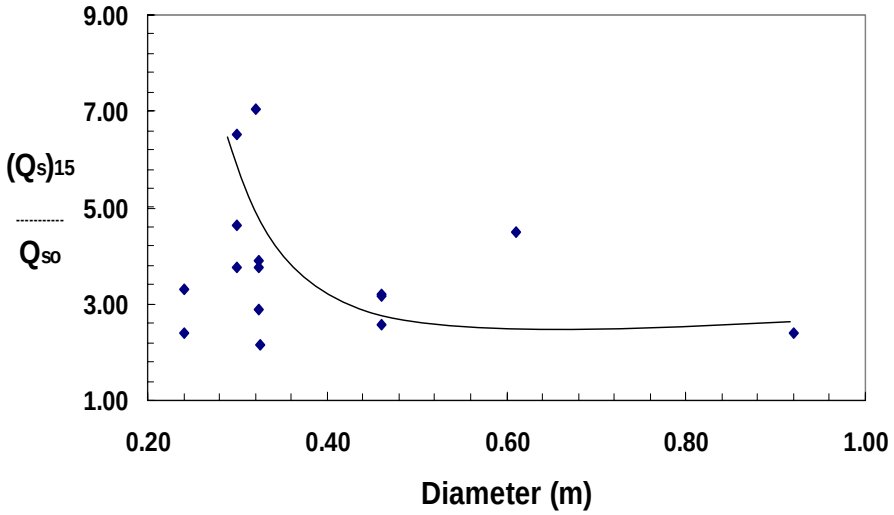

Figure (3-b): A Plot of $\frac{(Q_s)_{15}}{Q_{so}}$ versus pile diameter.

Figure (3): Normalized total and shaft capacity versus pile diameter.

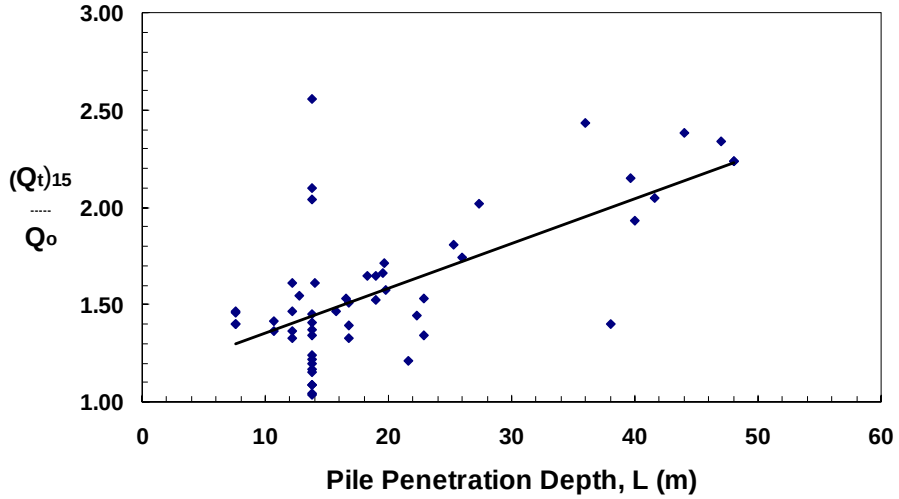

Figure (4-a): A Plot of $\frac{(Q_t)_{15}}{Q_o}$ versus pile embedded length (L).

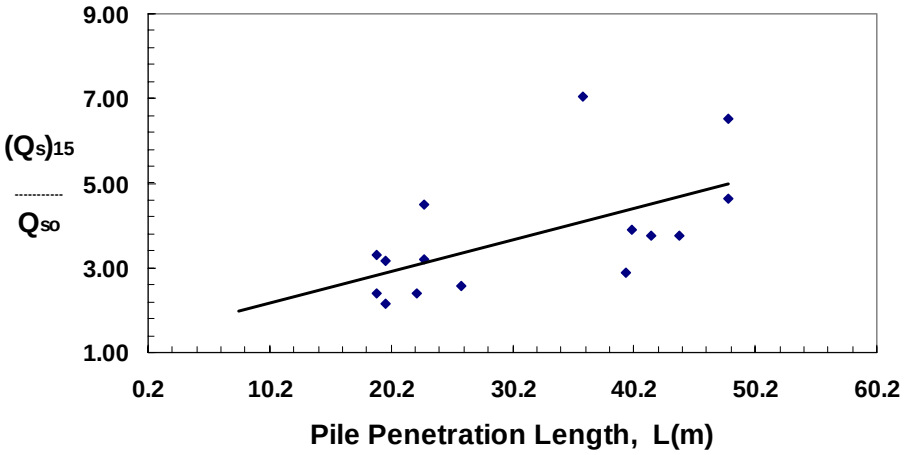

Figure (4-b): A Plot of $\frac{(Q_s)_{15}}{Q_{so}}$ versus pile embedded length (L).

Figure (4): Normalized total and shaft capacity versus pile length.

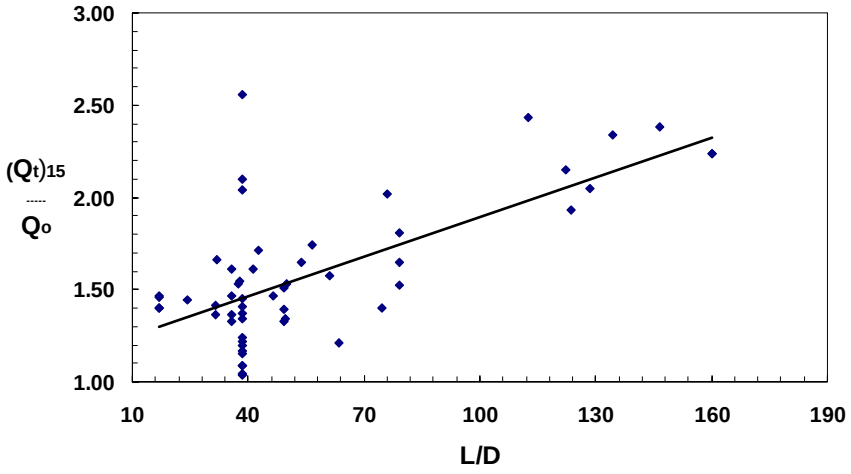

Figure (5-a): A Plot of $\frac{(Q_t)_{15}}{Q_o}$ versus (L/D).

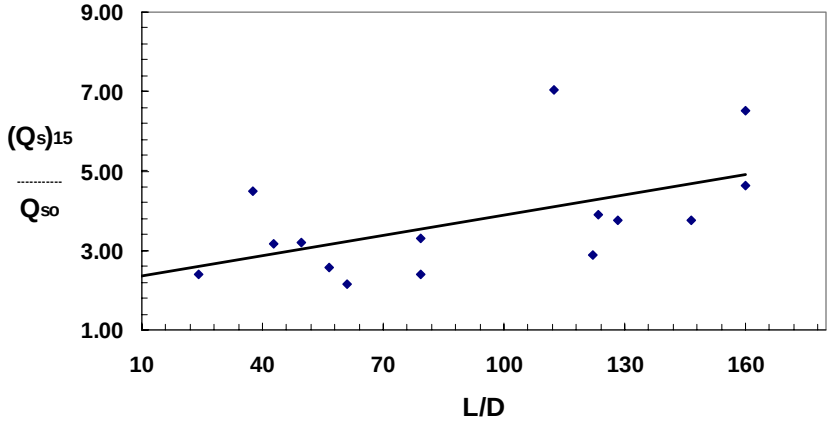

Figure (5-b): A Plot of $\frac{(Q_s)_{15}}{Q_{so}}$ versus (L/D).

Figure (5): Normalized total and shaft capacity versus (L/D).

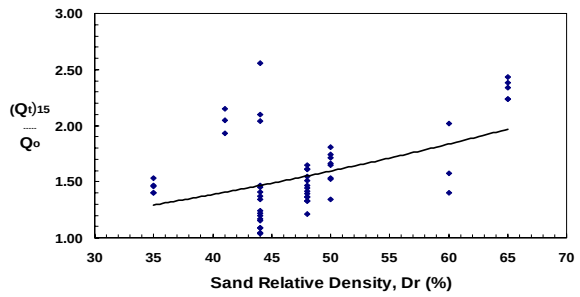

Figure (6-a): A Plot of $\frac{(Q_t)_{15}}{Q_o}$ versus sand relative density, Dr (%).

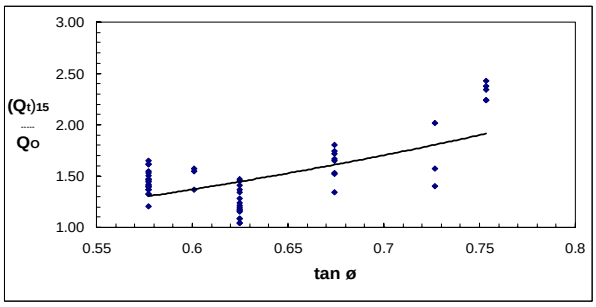

Figure (6-b): A Plot of $\frac{(Q_t)_{15}}{Q_o}$ versus coefficient of friction (tan ϕ) .

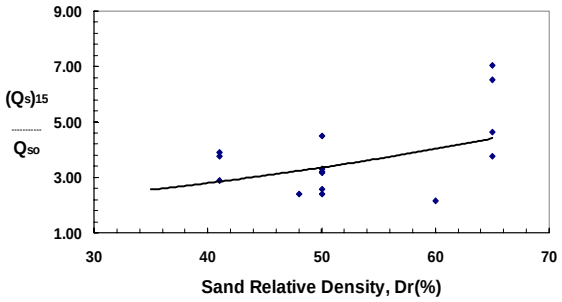

Figure (6-c): A Plot of $\frac{(Q_s)_{15}}{Q_{so}}$ versus sand relative density, Dr (%).

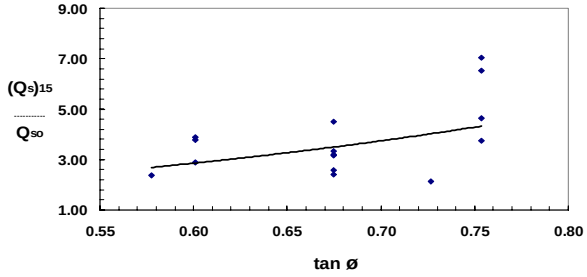

Figure (6-d): A Plot of $\frac{(Q_s)_{15}}{Q_{so}}$ versus coefficient of friction (tan ϕ).

Figure (6): Normalized total and shaft capacity versus soil relative density or coefficient of friction (tan ϕ).

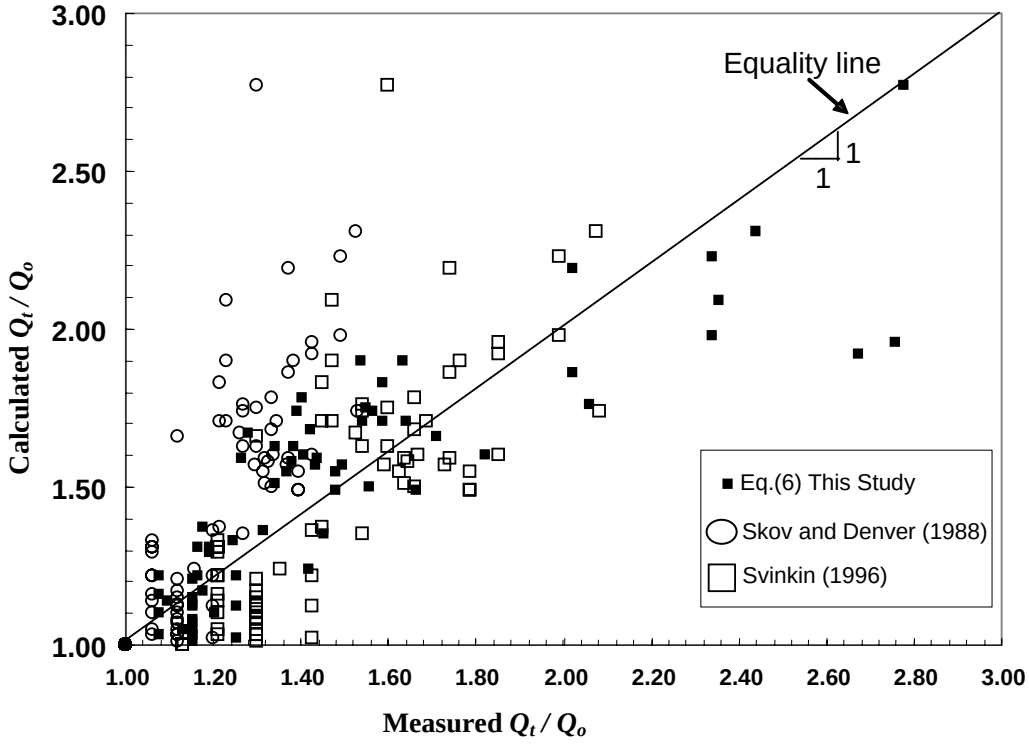

Figure (7): Comparison of prediction and measured set-up using different methods.

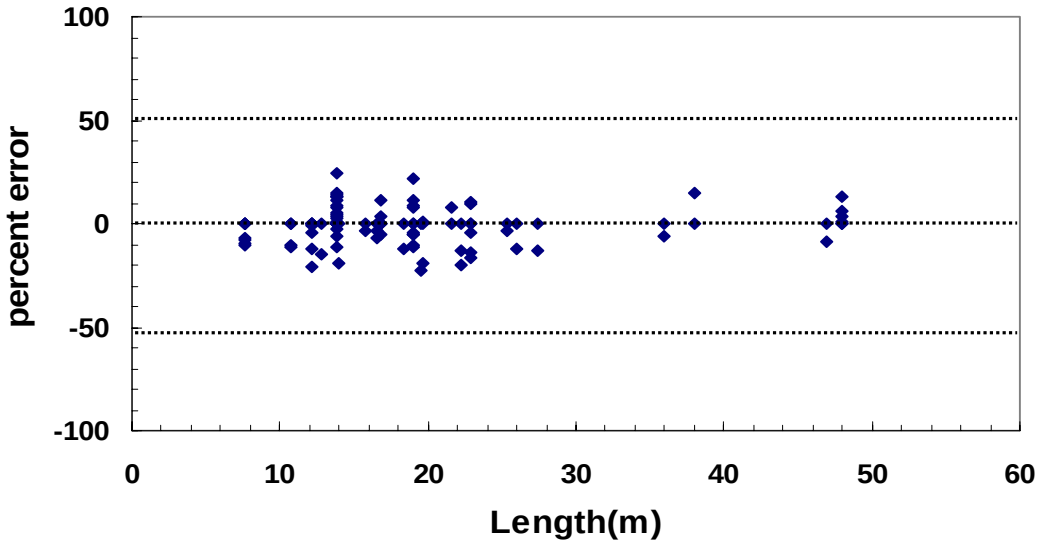

Figure (8): Percent error versus pile penetration depth [Eq. (6)].

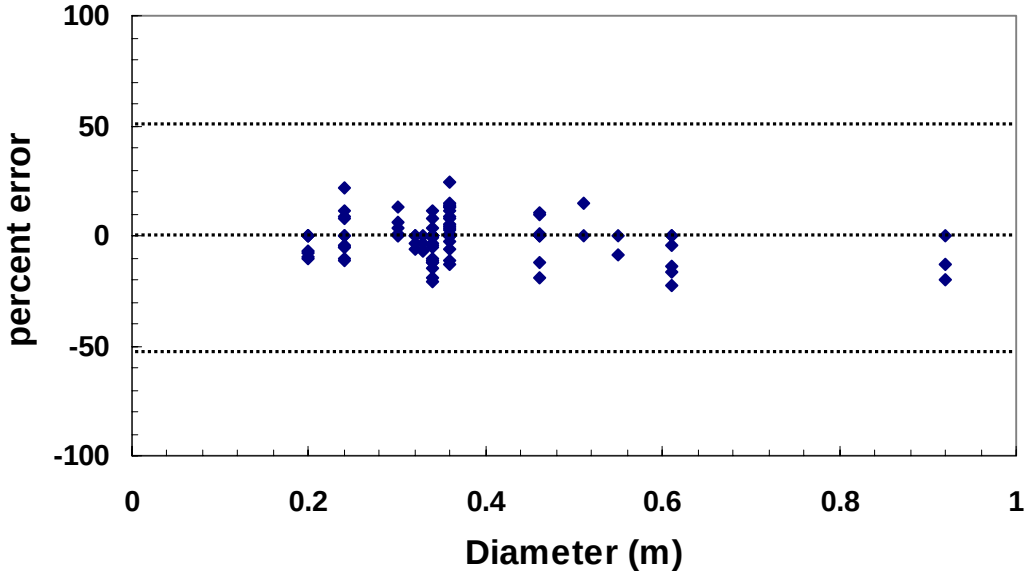

Figure (9): Percent error versus pile diameter [Eq. (6)].

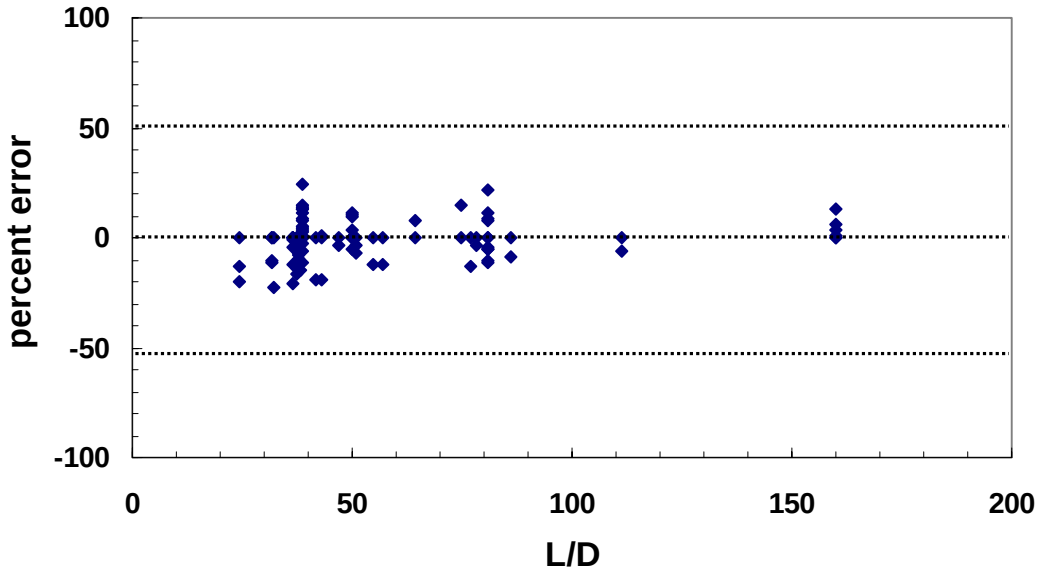

Figure (10): Percent error versus pile slenderness ratio [Eq. (6)].

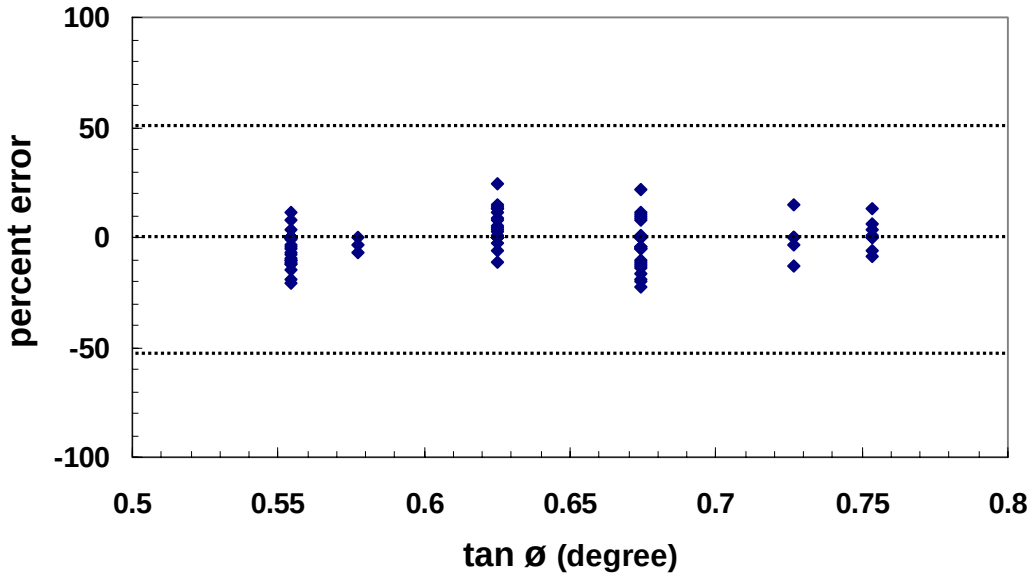

Figure (11): Percent error versus tan ϕ [Eq. (6)].

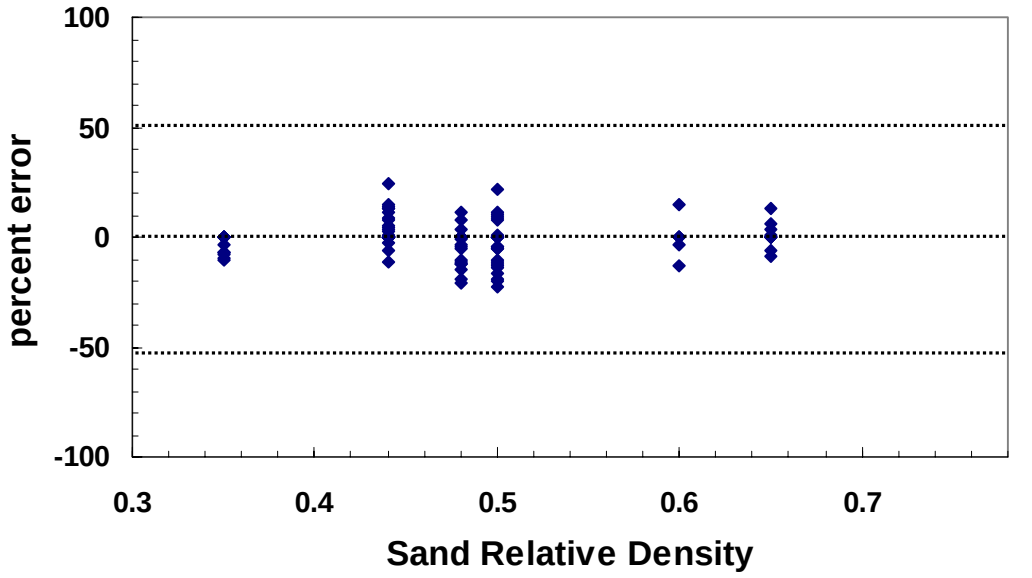

Figure (12): Percent error versus sand relative density [Eq. (6)].

Tan et al. (2004) modified equation (3) to:

$$Q(t) = Q_u \left[\alpha + (1-\alpha) \left[\frac{\frac{t}{T_{50}}}{1+\frac{t}{T_{50}}} \right] \right] \quad (4)$$

where α = empirical coefficient, probable lower bound = 0.2.

Tan et al. (2004) ensured that using hyperbolic function to estimate long-term pile set-up in cohesionless soil is more reliable than using the logarithm function.

Table (1): Collected database for this study (pile characteristics and load measurement with time).

Site Name and Reference	Serial No.	Pile No.	L (m)	D (mm)	L/D	Pile Type	Test	Pile Measured Capacity (kN)			Time after EOID (days)
								Total	Shaft	Toe	
Milwaukee Metropolitan Sewerage Fellenius et al. (1989)	1	A-2	36	320	112.5	Thin wall pile	EOID	943	516	427	0
							RSTR1	1877	1237	640	1
	2	B-2	48	300	160	H-pile	EOID	489	316	173	0
							RSTR1	1201	1023	178	2
							RSTR2	1512	1326	186	7
							RSTR4	2002	1686	316	16
	3	B-4	48	300	160	H-pile	EOID	645	467	178	0
							RSTR1	1219	1063	156	1
	4	B-3	44	300	146.6	H-pile	EOID	472	311	161	0
							RSTR1	1045	876	169	1
							STAT	907-1548	----	----	10
							RSTR4	1495	1241	254	13
	5	E-4	47	550	85.45	Heavy wall pipe (small diameter)	EOID	979	303	676	0
							RSTR1	1860	1286	574	1
JFK International Terminal, Jamaica, New York Fellenius and Altaee (2002)	6	1	7.6	450	16.8	Monotube piles	EOID	1910	----	----	0
							RSTR1	3020	----	----	19
	7	2	7.6	225	16.8	Monotube piles	EOID	2250	----	----	0
							RSTR1	3730	----	----	21
	8	3	7.6	450	16.8	Monotube piles	EOID	2530	----	----	0
							RSTR1	4010	----	----	35
	9	4	7.6	225	16.8	Steel-taper-tube pile	EOID	2360	----	----	0
							RSTR1	3820	----	----	37
North Shore, Vancouver Fellenius and Altaee (2002)	10	---	16.5	325	50	Pipe pile	EOID	900	----	----	0
							RSTR1	1200	----	----	1
							RSTR2	2400	1500	900	27
Southwest of Stockholm, Sweden Axelsson (2000)	11	A	19.8	235	79.17	Precast concrete piles	EOID	560	344	216	0
							RSTR1	703	492	378	0.0417
							RSTR2	890	595	295	1
							RSTR3	1247	746	501	6
							RSTR4	1354	1016	338	37
							RSTR5	1441	1079	344	143
	12	B	19.8	235	79.17	Precast concrete piles	EOID	529	274	225	0
							RSTR1	678	360	318	0.0278
							RSTR2	1006	875	130	1
							RSTR3	1402	1066	337	6
							RSTR4	1677	1188	489	37
							RSTR5	1710	1349	362	143
							RSTR6	1774	1365	409	216
	13	C	19.8	325	60.92	precast concrete piles	EOID	744	387	349	0
							RSTR	1441	1122	319	72
Svinkin (2002)	14	1	38	508	74.51	Prestressed concrete pile	EOID	2487	---	---	0
							RSTR1	3243	---	---	3
							STAT	6450	---	---	12
	15	2	27.4	356×356	76.11	Prestressed concrete pile	EOID	1134	---	---	0
							RSTR1	2309	---	---	7
							STAT	3736	---	---	16
	16	3	25.3	324	79.06	Thick closed end steel pipe	EOID	681	---	-----	----
							RSTR1	1232	---	---	7
							SLT	2224	---	---	14

Table (1): Continued

Site Name and Reference	Serial No.	Pile No.	L (m)	D (mm)	L/D	Pile Type	Test	Pile Measured Capacity (kN)			Time after EOID (days)
								Total	Shaft	Toe	
Svinkin (1996)	17	CT1	19.7	457×457	42.83	Prestressed concrete pile	EOID	913	334	579	0
							RSTR1	1145	668	447	2
							RSTR2	1702	---	---	11
	18	CT2	22.9	457×457	49.78	Prestressed concrete pile	EOID	1907	757	1140	0
							RSTR1	2176	1528	650	2
							RSTR2	2668	---	---	11
	19	CT3	19.5	610×610	31.97	Prestressed concrete pile	EOID	1513	695	811	0
							RSTR2	2615	---	---	10
	20	CT4	22.9	610×610	37.54	Prestressed concrete pile	EOID	1986	556	1421	0
							RSTR1	2691	1457	1234	2
							RSTR2	3617	---	---	11
							SLT	3724	---	---	23
	21	CT5	22.3	915×915	24.24	Prestressed concrete pile	EOID	2949	1310	1639	0
							RSTR1	4210	2807	1403	6
							STAT	4900	---	---	20
JFK International Airport, New York York et al. (1994)	22	P6	21.6	335	63.53	Hollow monotube pile	EOID	1246	---	---	0
							RSTR1	1380	---	---	1
	23	TP5	12.2	335	35.88	Hollow monotube pile	EOID	1041	---	---	0
							RSTR1	1558	---	---	48
	24	TP8	16.8	335	49.41	Hollow monotube pile	EOID	1202	---	---	0
							RSTR1	1802	---	---	48
	25	TP4	12.2	335	35.88	Concrete monotube	EOID	935	---	---	0
							RSTR1	1691	---	---	23
	26	TP10	12.2	335	35.88	Concrete monotube	EOID	1113	---	---	0
							RSTR1	1736	---	---	48
	27	TP7	16.8	335	49.41	Concrete monotube	EOID	1157	---	---	0
							RSTR1	1762	---	---	23
	28	T5-10	16.8	335	49.41	Monotube 3 gauge	EOID	1246	---	---	0
							RSTR1	1994	---	---	15
	29	J5-4	18.3	335	53.82	Monotube 3 gauge	EOID	1104	---	---	0
							RSTR1	1985	---	---	16
	30	LT2-172	12.2	335	35.88	Monotube 3 gauge	EOID	1073	---	---	0
							RSTR1	1744	---	---	24
	31	T5-107	12.8	335	37.65	Monotube 3 gauge	EOID	1179	---	---	0
							RSTR1	1958	---	---	16
	32	10B-4	14	335	41.18	Monotube 3 gauge	EOID	1090	---	---	0
							RSTR1	1922	---	---	42
	33	TP-11	10.7	335	31.47	Monotube 3 gauge	EOID	1046	---	---	0
							RSTR1	1602	---	---	20
	34	L-18-2	10.7	335	31.47	Timber	EOID	498	---	---	0
							RSTR1	868	---	---	224
	35	PP3	15.8	335	46.47	Pipe	EOID	2092	---	---	0
							RSTR1	2955	---	---	5
Downtown Lakeland, Polk country , West Central Florida Saxena (2004)	36	PP1	13.8	356	38.33	Precast prestressed concrete pile	EOID	922.7	---	---	0
							RSTR1	959.1	---	---	2
	37	PP2	13.8	356	38.33	Precast prestressed concrete pile	EOID	922.7	---	---	0
							RSTR1	959.1	---	---	2
	38	PP3	13.8	356	38.33	Precast prestressed concrete pile	EOID	822.7	---	---	0
							RSTR1	900	---	---	2
	39	PP4	13.8	356	38.33	Precast prestressed concrete pile	EOID	736.4	---	---	0
							RSTR1	1004.5	---	---	1

	40	PP6	13.8	356	38.33	Precast prestressed concrete pile	EOID	790.9	---	---	0
							RSTR1	877.3	---	---	2
	41	PP7	13.8	356	38.33	Precast prestressed concrete pile	EOID	2186.4	---	---	0
							RSTR1	2595.5	---	---	2
	42	PP8	13.8	356	38.33	Precast prestressed concrete pile	EOID	909.1	---	---	0
							RSTR1	959.1	---	---	1
	43	PP9	13.8	356	38.33	Precast prestressed concrete pile	EOID	763.6	---	---	0
							RSTR1	813.6	---	---	2
	44	PP10	13.8	356	38.33	Precast prestressed concrete pile	EOID	945.5	---	---	0
							RSTR1	1481.8	---	---	1
	45	PP12	13.8	356	38.33	Precast prestressed concrete pile	EOID	854.5	---	---	0
							RSTR1	1031.8	---	---	2
	46	PP13	13.8	356	38.33	Precast prestressed concrete pile	EOID	995.5	---	---	0
							RSTR1	1231.8	---	---	1
	47	PP15	13.8	356	38.33	Precast prestressed concrete pile	EOID	854.5	---	---	0
							RSTR1	995.5	---	---	2
	48	PP16	13.8	356	38.33	Precast prestressed concrete pile	EOID	764	---	---	0
							RSTR1	777	---	---	2
	49	PP17	13.8	35	38.33	Precast prestressed concrete pile	EOID	409	---	---	0
							RSTR1	514	---	---	5
	50	PP18	13.8	356	38.33	Precast prestressed concrete pile	EOID	1014	---	---	0
							RSTR1	1040	---	---	5
	51	PP19	13.8	356	38.33	Precast prestressed concrete pile	EOID	936	---	---	0
							RSTR1	1059	---	---	5
South Pylon Structure, Milwaukee, Wisconsin Komurka (2002)	52	Tp-1	41.6	324	128.4	Closed ended steel pipe	EOID	1805	239	1556	0
							RSTR1	2884	1327	1557	69
	53	Tp-17	39.6	324	122.2	Closed ended steel pipe	EOID	1735	371	1346	0
							RSTR1	3403	1528	1875	69
	54	Tp-18	40	324	123.4	Closed ended steel pipe	EOID	1450	255	1195	0
							RSTR1	2789	1471	1318	69
Central Florida Hussein et al. (2002)	55	---	26	457	56.52	Closed ended steel pipe	EOID	1155	585	570	0
							RSTR1	2115	1536	579	11
							STAT	2634	2055	579	17

Database for This Study

The database for this study is presented in Tables (1) and (2). Table (1) summarizes pile characteristics and measured pile capacity with time. Table (2) summarizes soil properties including relative density and friction angle of soil. The database consists of 55 pile load tests and comprises 5 closed - ended steel piles, 3 H-piles, 1 heavy wall pile, 1 thin wall pile, 15 monotube piles, 1 steel-taper-tube pile, 2 pipe piles, 26 precast concrete piles and 1 timber pile. These piles were driven into cohesionless soil of varying relative density from loose to dense soil (relative density of soil varies from 35% to 65%).

Table (2): Collected database for this study (soil properties).

Site Name and Reference	Soil Description	G.W.T. Location (m)	D_r (%)	ϕ (degree)
Milwaukee Metropolitan Sewerage Fellenius et al. (1989)	Silty sand to sandy silty and little clayey silt	8-	65	35-38
JFK International Terminal, Jamaica, New York Fellenius and Altaee (2002)	Thick deposit of fine to coarse, medium dense to dense glacial sand	No information	35	30
North Shore, Vancouver Fellenius and Altaee (2002)	The soil profile at the site consists of sand, gravel fill, silty sand, sandy silt, dense "till like" silt and sand until bedrock (sandstone)	-3.5	35	30
Southwest of Stockholm, Sweden Axelsson (2000)	Sweden, loose to medium dense saturated sand ,well graded varies between silty sand and gravelly sand	-2.0	30-50	32-35
Svinkin (2002)	Unsaturated sandy soils	No information	60	36
Svinkin (1996)	Dense saturated sand	-0.6	50	34
JFK International Airport, New York York et al. (1994)	Medium to fine sand fill and well–graded sand and fine gravel	-1.2 to -2.4	30-50	30
Downtown Lakeland, Polk Country, West Central Florida Saxena (2004)	Loose poorly graded sand underlain by layer of clayey sand in the upper 4.5m firm to hard elastic silty sand	-1.5 to - 3.5	44	32
South Pylon Structure, Milwaukee, Wisconsin Komurka (2002)	Fine to coarse sand	No information	41	31
Central Florida Hussein et al. (2002)	Dense to medium dense fine to coarse sand	-2.3	50	33

In most of the sites in Table (2), the GWT was very close to the ground surface. However, in some cases, no information was provided about the location of the GWT in the quoted references. The relative density values of the soils at most of the sites in Table (2) were obtained by converting field test data (SPT or CPT) to soil relative density using the correlations given by Peck et al. (1973). The friction angles shown in Table (2) for some of the sites were obtained from converting relative density to sand friction angle using the correlation proposed by Peck et al. (1973). The pile capacities were measured by performing either static or dynamic pile load test as indicated in Table (1).

Analysis of Database

From the database in Table (1), the following ratios are calculated and the results are summarized in Table (3): Q_t / Q_o, Q_s / Q_o, Q_s / Q_{so}, Q_p / Q_o and Q_p / Q_{po} where Q_o, Q_{so}, Q_{po} = total, shaft and point pile capacity, respectively after the End Of Initial Driving (EOID) and Q_t, Q_s, Q_p = total, shaft and point pile capacity at time (t) after the end of initial driving (upon restrike).

A plot of total pile capacity after each restrike to that after EOID versus time is shown in the Figure (2-a). Figure (2-a) indicates clearly that pile capacity in cohesionless soil increases with time and that this increase may continue up to a time longer than 200 days. The magnitude of the increase in pile capacity as indicated by the database of this study is, in some cases, significant and may reach as high as 400% of the initial pile capacity after the end of initial driving. This implies that the effect of set-up should be accounted for properly

in design. If the effect of set-up is considered, saving in pile penetration, diameter and reduction in size of driving equipment will be achieved. This, of course, results in cost saving in deep foundations.

As stated earlier, the time required for dissipation of excess pore water pressure in cohesionless soil resulting from pile driving is short. 12 to 24 hours is considered enough time to ensure complete dissipation of excess pore pressure (Castelli and Hussein, 1998). In most of the sites in this study, the GWT is very close to the ground surface. The increase in pile capacity up to time greater than 24 hours together with the magnitude of the observed set-up indicate that dissipation of excess pore water pressure doesn't account for the observed increase in pile capacity with time and other mechanisms contribute to the observed pile/soil set-up.

From Figure (2-b), the point resistance generally remains constant, slightly decreasing or increasing with time. On the other hand, shaft capacity as shown in Figure (2-c) increases with time. This clearly indicates that the increase in pile capacity with time primarily results from the increase in pile shaft capacity with time.

It should be stated that the scatter in the data shown in Figure (2-a) is attributed to the dependency of the magnitude of set-up on a combination of a number of influencing factors related to some extent to soil properties and pile characteristics.

Magnitude of Set-Up

As stated earlier, the magnitude of set-up is affected by many factors including pile diameter, pile penetration depth and soil friction angle or sand relative density.

In order to investigate the effect of these parameters on pile/soil set-up, the time at which the capacity of each pile in the database is measured should be theoretically fixed (i.e. time should be the same). In this study, pile capacity 15 days after the end of initial driving is selected to investigate the influence of the previously mentioned factors. For this purpose, only Equation (1) which was developed by Skov and Denver (1988) is adopted. The value of (*A*) in equation (1) which best fits the variation of measured capacity of each pile in the database is determined and the results are summarized in Table (4). The value of (*A*) for each pile in Table (4) is then used to compute pile capacities 15 days after the end of initial driving by applying Equation (1) using t_o =12 hours as shown by Skov and Denver (1988). The results are also summarized in Table (3) together with the normalized capacity ratio (pile capacity 15 days after the end of initial driving divided by pile capacity after the end of initial driving).

It should be stated that the time 15 days after EOID was selected in this analysis because most of the observed set-up by many investigators (Tavenas and Audy, 1972; Svinkin, 1996) was found to occur within 15 days after EOID.

Effect of Pile Diameter (D)

A plot of normalized total pile capacity 15 days after the end of initial driving with respect to pile capacity measured after the end of initial driving versus pile diameter is shown in Figure (3-a). The normalized total pile capacity $\frac{(Q_t)_{15}}{Q_O}$ is large for small pile diameter and decreases with increasing pile diameter. The same trend is observed when the normalized shaft capacity 15 days after the end of initial driving is plotted against pile diameter as shown in Figure (3-b). The result agrees with (Axelsson 2000), but disagrees with Long et al. (1999) who found no obvious difference in set-up between small and large displacement piles. Bowman and Soga (2005) confirmed that there is no greater effect of set-up for smaller diameter piles, the installation of larger piles will shear the soil to a greater extent.

Axelsson (2000) found that the magnitude and rate of set-up decreases as pile diameter increases. Axelsson (2000) stated that the soil parameters which affect the horizontal effective stress during pile loading as suggested by the cavity expansion theory are the stiffness of soil (shear modulus) and dilation. These parameters increase with time (soil aging) and this would lead to pile set-up. The effect of sand dilation on set-up decreases with increasing pile diameter (Chow et al., 1996):

Table (3): Analysis of database in this study.

Site Name and Reference	Serial No.	Pile No.	Test type	Time (day)	$\frac{Q_t}{Q_o}$	$\frac{Q_s}{Q_o}$	$\frac{Q_p}{Q_o}$	$\frac{Q_s}{Q_{so}}$	$\frac{Q_p}{Q_{po}}$
Milwaukee Metropolitan Sewerage Fellenius et al. (1989)	1	A-2	EOID	0	1.00	0.55	0.83	1.00	1.00
		A-2	RSTR1	1	1.99	1.31	1.24	2.40	1.50
	2	B-2	EOID	0	1.00	0.65	0.55	1.00	1.00
		B-2	RSTR1	2	2.46	2.09	0.56	3.24	1.03
		B-2	RSTR2	7	3.09	2.71	0.59	4.20	1.08
		B-2	RSTR4	16	4.09	3.45	1.00	4.20	1.08
	3	B-4	EOID	0	1.00	0.72	0.38	1.00	1.00
		B-4	RSTR1	1	1.89	1.65	0.33	2.28	0.88
	4	B-3	EOID	0	1.00			1.00	1.00
		B-3	RSTR1	1	2.21			2.82	1.05
		B-3	STAT	10	2.39				
		B-3	RSTR4	13	3.17			3.99	1.58
	5	E-4	EOID	0	1.00	0.31	2.23	1.00	1.00
		E-4	RSTR1	1	1.9	1.31	1.89	4.24	0.85
JFK International Terminal, Jamaica, New York Fellenius and Altaee (2002)	6	1	EOID	0	1.00				
		1	RSTR1	19	1.58				
	7	2	EOID	0	1.00				
		2	RSTR1	21	1.66				
	8	3	EOID	0	1.00				
		3	RSTR1	35	1.58				
	9	4	EOID	0	1.00				
		4	RSTR1	37	1.62				
North Shore, Vancouver Fellenius and Altaee (2002)	10	---	EOID	0	1.00				
		---	RSTR1	1	1.33				
		---	RSTR2	27	2.00				
Southwest of Stockholm, Sweden Axelsson (2000)	11	A	EOID	0	1.00	0.61	0.63	1.00	1.00
		A	RSTR1	0.05	1.26	0.88	1.10	1.43	1.75
		A	RSTR2	1	1.27	1.06	0.86	1.73	1.37
		A	RSTR3	6	2.23	1.33	1.46	2.17	2.32
		A	RSTR4	37	2.42	1.81	0.98	2.95	1.56
		A	RSTR5	143	2.57	1.93	1.00	3.14	1.59
	12	B	EOID	0	1.00	0.52	0.82	1.00	1.00
		B	RSTR1	0.03	1.21	0.68	1.16	1.31	1.41
		B	RSTR2	1	1.80	1.65	0.47	1.65	0.47
		B	RSTR3	6	2.65	2.02	1.23	2.02	1.23
		B	RSTR4	37	3.17	2.25	1.78	2.25	1.78
		B	RSTR5	143	3.23	2.55	1.32	2.55	1.32
		B	RSTR6	216	3.35	2.58	1.49	2.58	1.49
	13	C	EOID	0	1.00	0.52	0.90	0.52	0.90
		C	RSTR	72	1.94	1.51	0.82	1.51	0.82
Svinkin (2002)	14	1	EOID	0	1.00				
		1	RSTR1	3	1.30				
	15	2	EOID	0	1.00				
		2	RSTR1	7	2.04				
	16	3	EOID	0	1.00				
		3	RSTR1	7	1.81				

Tabe (3): continued

Site Name and Reference	Serial No.	Pile No.	Test type	Time (day)	$\frac{Q_t}{Q_o}$	$\frac{Q_s}{Q_o}$	$\frac{Q_p}{Q_o}$	$\frac{Q_s}{Q_{so}}$	$\frac{Q_p}{Q_{po}}$
Svinkin (1996)	17	CT1	EOID	0	1.00				
		CT1	RSTR1	2	1.25				
		CT1	RSTR2	11	1.86				
	18	CT2	EOID	0	1.00				
		CT2	RSTR1	2	1.14				
		CT2	RSTR2	11	1.40				
	19	CT3	EOID	0	1.00				
		CT3	RSTR2	10	1.73				
	20	CT4	EOID	0	1.00				
		CT4	RSTR1	2	1.35				
		CT4	RSTR2	11	1.82				
		CT4	SLT	23	1.88				
	21	CT5	EOID	0	1.00				
		CT5	RSTR1	6	1.43				
		CT5	SLT	20	1.66				
JFK International Airport, New York York et al. (1994)	22	P6	EOID	0	1.00				
		P6	RSTR1	1	1.11				
	23	TP5	EOID	0	1.00				
		TP5	RSTR1	48	1.50				
	24	TP8	EOID	0	1.00				
		TP8	RSTR1	48	1.50				
	25	TP4	EOID	0	1.00				
		TP4	RSTR1	23	1.81				
	26	TP10	EOID	0	1.00				
		TP10	RSTR1	48	1.56				
	27	TP7	EOID	0	1.00				
		TP7	RSTR1	23	1.52				
	28	T5-10	EOID	0	1.00				
		T5-10	RSTR1	15	1.60				
	29	J5-4	EOID	0	1.00				
		J5-4	RSTR1	16	1.80				
	30	LT-172	EOID	0	1.00				
		LT-172	RSTR1	24	1.63				
	31	T5-107	EOID	0	1.00				
		T5-107	RSTR1	16	1.66				
	32	10B-4	EOID	0	1.00				
		10B-4	RSTR1	42	1.76				
	33	TP-11	EOID	0	1.00				
		TP-11	RSTR1	20	1.53				
	34	L-18-2	EOID	0	1.00				
		L-18-2	RSTR1	224	1.74				
	35	PP3	EOID	0	1.00				
		PP3	RSTR1	5	1.41				

Table (3): continued

Site Name and Reference	Serial No.	Pile No.	Test type	Time (day)	$\frac{Q_t}{Q_o}$	$\frac{Q_s}{Q_o}$	$\frac{Q_p}{Q_o}$	$\frac{Q_s}{Q_{so}}$	$\frac{Q_p}{Q_{po}}$
Downtown Lakeland, Polk Country, West Central Florida. Saxena (2004)	36	PP1	EOID	0	1.00				
		PP1	RSTR1	2	1.04				
	37	PP2	EOID	0	1.00				
		PP2	RSTR1	2	1.04				
	38	PP3	EOID	0	1.00				
		PP3	RSTR1	2	1.09				
	39	PP4	EOID	0	1.00				
		PP4	RSTR1	1	1.36				
	40	PP6	EOID	0	1.00				
		PP6	RSTR1	2	1.11				
	41	PP7	EOID	0	1.00				
		PP7	RSTR1	2	1.19				
	42	PP8	EOID	0	1.00				
		PP8	RSTR1	1	1.05				
	43	PP9	EOID	0	1.00				
		PP9	RSTR1	2	1.07				
	44	PP10	EOID	0	1.00				
		PP10	RSTR1	1	1.57				
	45	PP12	EOID	0	1.00				
		PP12	RSTR1	2	1.21				
	46	PP13	EOID	0	1.00				
		PP13	RSTR1	1	1.24				
	47	PP15	EOID	0	1.00				
		PP15	RSTR1	2	1.17				
	48	PP16	EOID	0	1.00				
		PP16	RSTR1	2	1.02				
	49	PP17	EOID	0	1.00				
		PP17	RSTR1	5	1.26				
	50	PP18	EOID	0	1.00				
		PP18	RSTR1	5	1.03				
	51	PP19	EOID	0	1.00				
		PP19	RSTR1	5	1.13				
South Pylon Structure, Milwaukee, Wisconsin Komurka (2002)	52	TP-15	EOID	0	1.00	0.13	6.55	0.13	6.55
		TP-15	RSTR1	69	1.60	0.74	6.51	0.74	6.51
	53	TP-17	EOID	0	1.00	0.21	3.68	0.21	3.68
		TP-17	RSTR1	69	1.96	0.88	5.05	0.88	5.05
	54	TP-18	EOID	0	1.00	0.07	0.78	0.07	0.78
		TP-18	RSTR1	69	1.92	1.01	5.17	1.01	5.17
Central Florida Hussein et al. (2002)	55	***	EOID	0	1.00	0.51	0.97	0.51	0.97
		***	RSTR1	11	1.83	1.33	0.99	1.33	0.99
		***	STAT	17	2.28	1.78	0.99	1.78	0.99

Table (4): Calculation of pile capacity 15 days after (EOID) using equation (1).

Site Name and Reference	Serial No.	Pile No.	Calculated (A)		Calculated Capacity 15days after (EOID)		$\frac{(Q_t)_{15}}{Q_o}$	$\frac{(Q_s)_{15}}{Q_{so}}$
			Total Capacity	Shaft Capacity	Total Capacity $(Q_t)_{15}$	Shaft Capacity $(Q_s)_{15}$		
Milwaukee Metropolitan Sewerage Fellenius et al. (1989)	1	A-2	1.10	4.64	3714.14	4053.846	2.62	7.85
	2	B-2	0.95	2.79	1739.96	1617.692	2.40	5.12
	3	B-4	0.95	4.24	2278.30	3391.513	2.40	7.26
	4	B-3	1.06	2.11	1211.03	1281.798	2.57	4.12
	5	E-4	1.03	10.78	3580.44	5126.489	2.52	16.92
JFK International Terminal, Jamaica, New York Fellenius and Altaee (2002)	6	1	0.35		2955.40		1.52	
	7	2	0.36		3495.76		1.53	
	8	3	0.31		3719.06		1.46	
	9	4	0.31		3469.82		1.46	
North Shore, Vancouver Fellenius and Altaee (2002)	10	---	0.41		1689.11		1.61	
Southwest of Stockholm, Sweden Axelsson (2000)	11	A	0.40	1.08	1158.14	894.1627	1.59	2.60
	12	B	0.50	1.78	1333.48	996.2075	1.74	3.63
	13	C	0.44	0.88	1227.55	890.0176	1.65	2.30
Svinkin (2002)	14	1	0.31		3806.60		1.46	
	15	2	0.78		2621.32		2.15	
	16	3	0.62		1379.39		1.92	
Svinkin (1996)	17	CT1	0.55	1.66	1770.73	1153.431	1.81	3.45
	18	CT2	0.26	1.69	2737.65	2648.533	1.38	3.50
	19	CT3	0.51		2750.98		1.75	
	20	CT4	0.41	2.69	3562.87	2766.521	1.61	4.97
	21	CT5	0.34	1.06	4622.33	3359.114	1.50	2.57
JFK International Airport, New York York et al. (1994)	22	P6	0.16		1625.79		1.24	
	23	TP5	0.25		1433.64		1.37	
	24	TP8	0.25		1655.46		1.37	
	25	TP4	0.47		1612.92		1.69	
	26	TP10	0.28		1583.23		1.41	
	27	TP7	0.30		1689.91		1.44	
	28	T5-10	0.39		2003.19		1.58	
	29	J5-4	0.50		1968.05		1.74	
	30	LT-172	0.36		1666.56		1.53	
	31	T5-107	0.42		1950.95		1.62	
	32	10B-4	0.47		1711.19		1.69	
	33	TP-11	0.32		1561.04		1.47	
	34	L-18-2	0.28		705.38		1.41	
	35	PP3	0.36		3334.65		1.53	

Table (4): Continued

Site Name and Reference	Serial No.	Pile No.	Calculated (A)		Calculated Capacity 15days after (EOID)		$\frac{(Q_t)_{15}}{Q_o}$	$\frac{(Q_s)_{15}}{Q_{so}}$
			Total Capacity	Shaft Capacity	Total Capacity $(Q_t)_{15}$	Shaft Capacity $(Q_s)_{15}$		
Downtown Lakeland Polk Country, West Central Florida Saxena (2004)	36	PP1	0.05		1000.83		1.07	
	37	PP2	0.05		1000.83		1.07	
	38	PP3	0.12		990.07		1.18	
	39	PP4	0.52		1536.48		1.77	
	40	PP6	0.13		969.12		1.19	
	41	PP7	0.22		3035.50		1.32	
	42	PP8	0.10		1069.67		1.15	
	43	PP9	0.08		868.82		1.12	
	44	PP10	0.73		2525.13		2.08	
	45	PP12	0.24		1219.06		1.35	
	46	PP13	0.35		1691.45		1.52	
	47	PP15	0.19		1141.06		1.28	
	48	PP16	0.02		790.69		1.03	
	49	PP17	0.22		556.49		1.32	
	50	PP18	0.02		1047.04		1.03	
South Pylon Structure, Milwaukee, Wisconsin Komurka (2002)	51	PP19	0.12		1116.04		1.18	
	52	TP-15	0.28	2.13	619.15		1.41	4.15
	53	TP-17	0.44	1.46	694.62	990.0617	1.65	3.16
	54	TP-18	0.42	2.23	570.38	1169.719	1.62	4.29
Apalachicola River Florida Hussein et al. (2002)	55	***	0.57	1.21	2208.51	1094.403	1.84	2.79

Table (5): Error analysis.

Corr. No.	Correlation	Reference	Mean error (%)	Max. Error (%)	Min. Error (%)	Error Range (%)	Error St. Dev. (%)
1	$Q_t/Q_o=1+0.005*(L/D)*\exp(0.6*\tan\phi)*\log(t/t_o)$ $R^2=0.870$	This study	-1	23.9	-22.2	46.1	8.36
2	$Q_t/Q_o=1+0.007*(L/D)*\exp(0.14*D_r)*\log(t/t_o)$ $R^2=0.872$	This study	1.02	23.3	-22.6	45.9	8.29
3	$Q_t/Q_o=1+0.007*(L/D)*\log(t/t_o)$ $R^2=0.879$	This study	-0.69	24.8	22.2	47	8.1
4	$Q_s/Q_o=1+0.009*\log(t/t_o)*\exp(0.29*\tan\phi)*(L/D)$ $R^2=0.79$	This study	-3.42	44.8	-46.7	91.5	20.85
5	$Q_s/Q_o=1+0.01*\log(t/t_o)*\exp(0.16*Dr)*(L/D)$ $R^2=0.77$	This study	-1.7	46.1	-46.6	92.7	22.08
6	$Q_s/Q_o=1+0.012*(L/D)*\log(t/t_o)$ $R^2=0.801$	This study	-3.42	46.8	-39.2	86	17.3
7	$Q_t/Q_o=(1.4to1.025)*t^{0.1}$ $R^2=0.737$	Svinkin (1996)	-8.35	18.6	-50.7	69.3	10.74
8	$Q_t/Q_o=1+0.2*\log(t/t_o)$ $R^2=0.746$	Skov & Denver (1988)	-7.96	17.3	52.9	70.2	12.73

Table (6): Comparison of predicted and measured set-up using different methods.

Site Name and Reference	Pile No.	Time (day)	$(Q_t/Q_o)_{measured}$	$(Q_t/Q_o)_{calculated}$			
				This study		Skov& Denver (1988)	Svinkin (1996)
				Equation (6)	Equation (7)		
Milwaukee Metropolitan Sewerage Fellenius et al. (1989)	A-2	0.50	1.00	1.00	1.00	1.00	1.13
	A-2	1.00	1.33	1.26	1.25	1.06	1.21
	B-2	0.50	1.00	1.00	1.00	1.00	1.13
	B-2	2.00	1.66	1.76	1.71	1.12	1.30
	B-2	7.00	2.09	2.44	2.35	1.23	1.47
	B-2	16.00	2.77	2.89	2.78	1.30	1.60
	B-4	0.50	1.00	1.00	1.00	1.00	1.13
	B-4	0.50	1.00	1.00	1.00	1.00	1.13
	E-4	1.00	1.31	1.20	1.19	1.06	1.21
	E-4	1.00	1.29	1.20	1.19	1.06	1.21
JFK International Terminal, Jamaica, New York Fellenius and Altaee (2002)	1	0.50	1.00	1.00	1.00	1.00	1.13
	1	19.00	1.55	1.42	1.37	1.32	1.63
	2	0.50	1.00	1.00	1.00	1.00	1.13
	2	21.00	1.58	1.43	1.38	1.32	1.64
	3	0.50	1.00	1.00	1.00	1.00	1.13
	3	35.00	1.57	1.49	1.43	1.37	1.73
	4	0.50	1.00	1.00	1.00	1.00	1.13
	4	37.00	1.59	1.50	1.44	1.37	1.74
North Shore, Vancouver Fellenius and Altaee (2002)	---	0.50	1.00	1.00	1.00	1.00	1.13
	---	1.00	1.14	1.11	1.09	1.06	1.21
	---	27.00	1.71	1.62	1.54	1.35	1.69
Southwest of Stockholm, Sweden Axelsson (2000)	A	0.50	1.00	1.00	1.00	1.00	1.13
	A	1.00	1.22	1.18	1.16	1.06	1.21
	A	6.00	1.71	1.65	1.59	1.22	1.45
	A	37.00	1.86	2.13	2.02	1.37	1.74
	A	143.00	1.98	2.49	2.34	1.49	1.99
	B	0.50	1.00	1.00	1.00	1.00	1.13
	B	1.00	1.31	1.18	1.16	1.06	1.21
	B	6.00	1.83	1.65	1.59	1.22	1.45
	B	37	2.19	2.13	2.02	1.37	1.74
	B	143.	2.23	2.49	2.34	1.49	1.99
	B	216.	2.31	2.60	2.44	1.53	2.08
Svinkin (2002)	1	0.50	1.00	1.00	1.00	1.00	1.13
	1	3.00	1.24	1.45	1.42	1.16	1.35
	2	0.50	1.00	1.00	1.00	1.00	1.13
	2	7.00	1.90	1.68	1.63	1.23	1.47
	3	0.50	1.00	1.00	1.00	1.00	1.13
	3	7.00	1.71	1.69	1.64	1.23	1.47

Table (6): Continued

Site Name and Reference	Pile No.	Time (day)	$(Q_t/Q_o)_{measured}$	$(Q_t/Q_o)_{calculated}$			
				This study		Skov & Denver (1988)	Svinkin (1996)
				Equation (6)	Equation (7)		
Svinkin (1996)	CT1	0.50	1.00	1.00	1.00	1.00	1.13
	CT1	2.00	1.17	1.19	1.18	1.12	1.30
	CT1	11.00	1.74	1.43	1.39	1.27	1.54
	CT2	0.50	1.00	1.00	1.00	1.00	1.13
	CT2	2.00	1.10	1.23	1.20	1.12	1.30
	CT2	11.00	1.35	1.50	1.45	1.27	1.54
	CT3	0.50	1.00	1.00	1.00	1.00	1.13
	CT3	0.50	1.00	1.00	1.00	1.00	1.13
	CT3	10.00	1.67	1.31	1.28	1.26	1.53
	CT4	0.50	1.00	1.00	1.00	1.00	1.13
	CT4	2.00	1.21	1.17	1.15	1.12	1.30
	CT4	11.00	1.63	1.38	1.34	1.27	1.54
	CT4	23.00	1.68	1.47	1.42	1.33	1.66
	CT5	0.50	1.00	1.00	1.00	1.00	1.13
	CT5	6.00	1.37	1.20	1.18	1.22	1.45
	CT5	20.00	1.59	1.29	1.26	1.32	1.64
JFK International Airport, New York York et al. (1994)	P6	0.50	1.00	1.00	1.00	1.00	1.13
	P6	1.00	1.05	1.14	1.13	1.06	1.21
	TP5	0.50	1.00	1.00	1.00	1.00	1.13
	TP5	48.00	1.49	1.50	1.48	1.40	1.79
	TP8	0.50	1.00	1.00	1.00	1.00	1.13
	TP8	48.00	1.49	1.69	1.66	1.40	1.79
	TP4	0.50	1.00	1.00	1.00	1.00	1.13
	TP4	23.00	1.78	1.42	1.40	1.33	1.66
	TP10	0.50	1.00	1.00	1.00	1.00	1.13
	TP10	48.00	1.55	1.50	1.48	1.40	1.79
	TP7	0.50	1.00	1.00	1.00	1.00	1.13
	TP7	23.00	1.50	1.58	1.56	1.33	1.66
	T5-10	0.50	1.00	1.00	1.00	1.00	1.13
	T5-10	15.00	1.57	1.52	1.49	1.30	1.59
	J5-4	0.50	1.00	1.00	1.00	1.00	1.13
	J5-4	16.00	1.75	1.57	1.55	1.30	1.60
	LT-172	0.50	1.00	1.00	1.00	1.00	1.13
	LT-172	24.00	1.60	1.43	1.41	1.34	1.67
	T5-107	0.50	1.00	1.00	1.00	1.00	1.13
	T5-107	16.00	1.63	1.40	1.38	1.30	1.60
	10B-4	0.50	1.00	1.00	1.00	1.00	1.13
	10B-4	42.00	1.90	1.56	1.54	1.38	1.76
	TP-11	0.50	1.00	1.00	1.00	1.00	1.13
	TP-11	20.00	1.51	1.36	1.34	1.32	1.64

	L-18-2	0.50	1.00	1.00	1.00	1.00	1.13
	L-18-2	224.00	1.74	1.59	1.56	1.53	2.08
	PP3	0.50	1.00	1.00	1.00	1.00	1.13
	PP3	5.00	1.36	1.33	1.31	1.20	1.42
	PP6	0.50	1.00	1.00	1.00	1.00	1.13
Downtown Lakeland, Polk Country, West Central Florida Saxena (2004)	PP6	2.00	1.08	1.17	1.15	1.12	1.30
	PP7	0.50	1.00	1.00	1.00	1.00	1.13
	PP7	2.00	1.13	1.17	1.15	1.12	1.30
	PP8	0.50	1.00	1.00	1.00	1.00	1.13
	PP8	1.00	1.03	1.08	1.08	1.06	1.21
	PP9	0.50	1.00	1.00	1.00	1.00	1.13
	PP9	2.00	1.05	1.17	1.15	1.12	1.30
	PP10	0.50	1.00	1.00	1.00	1.00	1.13
	PP10	1.00	1.22	1.08	1.08	1.06	1.21
	PP12	0.50	1.00	1.00	1.00	1.00	1.13
	PP12	2.00	1.15	1.17	1.15	1.12	1.30
	PP13	0.50	1.00	1.00	1.00	1.00	1.13
	PP13	1.00	1.10	1.08	1.08	1.06	1.21
	PP15	0.50	1.00	1.00	1.00	1.00	1.13
	PP15	2.00	1.12	1.17	1.15	1.12	1.30
	PP16	0.50	1.00	1.00	1.00	1.00	1.13
	PP16	2.00	1.01	1.17	1.15	1.12	1.30
	PP17	0.50	1.00	1.00	1.00	1.00	1.13
	PP17	5.00	1.22	1.28	1.25	1.20	1.42
	PP18	0.50	1.00	1.00	1.00	1.00	1.13
	PP18	5.00	1.02	1.28	1.25	1.20	1.42
	PP19	0.50	1.00	1.00	1.00	1.00	1.13
	PP19	5.00	1.12	1.28	1.25	1.20	1.42
South Pylon Structure, Milwaukee, Wisconsin Komurka (2002)	TP-15	0.50	1.00	1.00	1.00	1.00	1.13
	TP-15	69.00	1.60	1.91	1.82	1.43	1.85
	TP-17	0.50	1.00	1.00	1.00	1.00	1.13
	TP-17	69.00	1.96	2.87	2.76	1.43	1.85
	TP-18	0.50	1.00	1.00	1.00	1.00	1.13
	TP-18	69.00	1.92	2.78	2.67	1.43	1.85
Central Florida Hussein et al. (2002)	***	0.50	1.00	1.00	1.00	1.00	1.13
	***	11.00	1.76	2.13	2.06	1.27	1.54

$$\Delta\sigma'_{rd} = \frac{4.G.R_{cal}}{R} \quad (5)$$

where

$\Delta\sigma'_{rd}$ = Increase in radial stress during loading due to sand dilation.

G = Sand shear modulus.

R_{cal} = Center-line average roughness of the pile surface.

R = Pile radius.

Equation (5) may provide a theoretical framework explanation, where the increase in radial stress on the pile shaft is proportional to sand shear modulus (G) and inversely proportional to pile radius (R).

Effect of Pile Penetration Depth (L)

A plot of normalized total pile capacity 15 days after the end of initial driving with respect to pile capacity measured after the end of initial driving versus pile penetration depth is shown in Figure (4-a).

Generally, the magnitudes of set-up increase with increasing pile penetration depth. Since shaft capacity acts along the pile embedded depth, the trend in Figure (4-a) may indicate that shaft capacity plays an important role in controlling the magnitude of set-up as percentage. This is obvious when the normalized shaft capacity 15 days after the end of initial driving with respect to that measured at the end of initial driving is plotted against pile penetration depth as shown in Figure (4-b). The conclusion that set-up is derived from shaft capacity rather than toe capacity is also made from Figure (2-b) which shows no significant increase in toe capacity with time.

Saxena (2004) observed that longer piles generally exhibit higher set-ups than shorter piles, longer piles have greater surface areas than shorter piles of the same diameter. Moreover, longer piles exhibit higher confining pressure due to the overburden.

Effect of Pile Slenderness Ratio (L/D)

The combined effect of pile diameter and penetration depth can be investigated by plotting the normalized total pile capacity 15 days after the end of initial driving with respect to pile capacity after the end of initial driving versus *(L/D)* as shown in Figure (5-a). In general, set-up as percentage increases with increasing *(L/D)* ratio. The same trend is obvious when $\frac{(Q_s)_{15}}{Q_{so}}$ is plotted against *(L/D)* as shown in Figure (5-b).

Effect of Sand Relative Density

As shown in Figure (6-a) and (6-b), the ratio $\frac{(Q_t)_{15}}{Q_o}$ increases slightly with increasing sand relative density or sand friction angle. Similar trend is obtained when $\frac{(Q_s)_{15}}{Q_{so}}$ is plotted against soil relative density or tan ϕ where ϕ is the friction angle of soil as shown in Figure (6-c) and (6-d). Schmertmann (1991) suggested that the increases in soil stiffness and strength due to aging have resulted entirely from an increased friction capability. The contribution of sand dilation during loading (Equation 5) is significant when the soil is initially dense.

Proposed Correlations to Estimate Set-Up

In a normalized way, the ratio of total pile capacity at time (*t*) to that after end of initial driving (Q_t / Q_o) for the database in Table (1) are correlated to pile slenderness ratio ($\frac{L}{D}$) and the coefficient of friction (tan ϕ) as follows:

$$\frac{Q_t}{Q_o} = 1 + 0.005\left(\frac{L}{D}\right)\exp(0.6\tan\phi)\log\left(\frac{t}{t_o}\right) \quad (6)$$

Also the ratio of total pile capacity at time (*t*) to that after the end of initial driving (Q_t / Q_o) for the database in Table (1) are correlated to pile slenderness ratio ($\frac{L}{D}$) and sand relative density as follows:

$$\frac{Q_t}{Q_o} = 1 + 0.007\left(\frac{L}{D}\right)\exp(0.14 D_r)\log\left(\frac{t}{t_o}\right) \quad (7)$$

If the soil relative density (*Dr*) is available rather than the friction angle of soil (ϕ), the correlation in equation (7) can be used instead.

The statistical analysis of the collected database indicates that the normalized pile penetration depth with respect to pile diameter *(L/D)* is the most significant factor influencing the magnitude of set-up. The effect of soil friction angle seems to be insignificant in comparison to the normalized penetration depth, as such, the ratio of total pile capacity at time (*t*) to that after the end of initial driving (Q_t /Q_o) for the database in Table (1) is correlated to pile slenderness ratio (*L/D*) only to get the following simpler empirical equation:

$$\frac{Q_t}{Q_o} = 1 + 0.007\left(\frac{L}{D}\right)\log\left(\frac{t}{t_o}\right) \quad (8)$$

Another set of similar correlations are obtained in this study by correlating the ratio of shaft capacity at time (t) to that after the end of initial driving (Q_s /Q_{so}) for the database in Table (1) to pile slenderness ratio and the coefficient of friction ($\tan\phi$) or sand relative density:

$$\frac{Q_s}{Q_{so}} = 1 + 0.009\,(\frac{L}{D})\exp(0.29\tan\phi)\log(\frac{t}{t_o}) \qquad (9)$$

$$\frac{Q_s}{Q_{so}} = 1 + 0.01(\frac{L}{D})\exp(0.16\,D_r)\log(\frac{t}{t_o}) \qquad (10)$$

The ratio of shaft capacity at time (t) to that after the end of initial driving (Q_s /Q_{so}) for the database in Table (1) is also correlated to pile slenderness ratio only to get the following simple correlation:

$$\frac{Q_s}{Q_{so}} = 1 + 0.012\,(\frac{L}{D})\log(\frac{t}{t_o}) \qquad (11)$$

Error Analysis

The proposed correlations in this study are developed for use in estimating the increase in pile capacity with time for driven piles in cohesionless soil. To evaluate the accuracy of these correlations in estimating set-up, it is necessary to perform an error analysis. The analysis allows us to evaluate the accuracy of each correlation separately and also compare results using correlations developed by others.

The percent error is defined as the difference between predicted pile set-up using the developed relationships and the measured set-up divided by the measured set-up as follows:

$$\%Erorr = \frac{\Pr edicted - Measured}{Measured} \times 100\%$$

The percent error in predicted pile set-up using the proposed correlations and the arithmetic mean error and standard deviation were calculated, and the results are summarized in Table (5). Positive mean error means that the relationship overestimates pile set-up and negative mean error implies that the relationship underpredicts the data.

From the statistics summarized in Table (5), it can be stated that the first three correlations are not significantly different from each other in predicting set-up.

As shown in Table (5), comparison of the percent error in predicted set-up for the database in this study using Skov and Denver (1988) method and Svinkin (1996) method with those made using the proposed correlations in this study indicates that the first three correlations in Table (5) yield better results (see also Figure (7) and Table (6)).

From Table (6), it seems that Equation (6) is the best correlation which can predict pile set-up. To evaluate the dependency of the calculated percent error on sand relative density, friction angle, pile diameter, pile penetration depth and pile slenderness ratio, plots of percent error are prepared and shown in Figures (8) through (12) for the first correlation in Table (5). In general, the first correlation in Table (5) gives good prediction in loose as well as in dense sands. It also yields good set-up prediction for long and short piles.

Estimation of Total Pile Capacity Considering Set-Up

From the analysis of the database in this study, it can be stated that equation (6) yields good prediction for long and short piles. In this study, a method is proposed for estimating total pile capacity considering pile set-up using equation (6) as follow:

$$Q_t = Q_o\,(1 + A\log(\frac{t}{t_o})) \qquad (12\text{-a})$$

where

$$A = 0.005\,(\frac{L}{D})\exp(0.6\tan\phi) \qquad (12\text{-b})$$

t_o = 12 hours = 0.5 day (12-c)

In equation (12-a), Q_o can be estimated from the method of Alawneh et al. (2001) as follow:

$$Q_o = Q_S + Q_P \qquad (13)$$

where

Q_o = Total pile capacity at EOID.

Q_s = Shaft pile capacity at EOID.
Q_p = Pile point capacity at EOID.

Estimation of Shaft Resistance (Q_s)

$$Q_S = A_s \sigma'_v (\beta)_{adj.} \quad (14)$$

$$(\beta)_{adj.} = 1.54 \exp(0.016 D_r)(\sigma'_v)^{-0.45} \quad (15)$$

where
A_s = Pile unit circumferential surface area.

σ'_v = Average effective overburden pressure along the pile.
$\beta_{adj.}$ = Bjerrum-Burland ratio adjusted for residual load.

D_r = Relative density of soil.

Estimation of Point Resistance (Q_p)

$$Q_p = q'_o (N_q)_{adj.} (A_t) \quad (16)$$

$$(N_q)_{adj.} = 5.32 \exp(-2.72 \sin\phi) I_{rr}^{1.68 \sin\phi} \sin\phi \quad (17)$$

where:
q'_o = effective vertical stress at pile end point.
ϕ = friction angle of soil at the pile end point (degree).
I_{rr} = reduced rigidity index of soil.
A_t = Area of the pile toe.

$(N_q)_{adj.}$ = Bearing capacity factor adjusted for residual load.

More details may be found in Alwaneh et al. (2001).

Set-Up and Cost Saving Aspect

Using a design method that considers set-up leads under certain conditions to considerable saving in deep foundation cost. Pile length, diameter and driving energy will be reduced if the increase in pile capacity with time is considered in design. This aspect is illustrated in the following example.

Example

It's necessary to find the required embedded length of circular pile (closed ended with outside diameter of 0.4 m) to carry a working load of 1000 kN. The pile is driven into a medium dense sand layer (relative density = 50%). The unit weight of sand is 19 kN/m³ (γ' = 9.19 kN/m³) and the GWT coincides with the ground surface, soil friction angle = 33º, c = 0, and the reduced rigidity index I_{rr} = 130.

Solution

Ignoring pile set-up

Using equation (14) and (15) to find shaft capacity

$$\beta_{adj.} = 1.54\, exp\,(0.016\ x\,0.5)\left(\frac{L}{2} x\, 9.19\right)^{-0.45} = 0.789\ L^{-0.45}$$

$$Q_s = [\pi\,(0.4)\,L]\left[\frac{L}{2} x\, 9.19\right][0.789\ L^{-0.45}] = 5.68\, L^{1.55}$$

Using Equations (16) and (17) to find end point capacity

$$(N_q)_{adj.} = 5.32\ exp\,[-2.72\ sin\,(33)]\ [130.0]^{1.68\ sin\,(33)}\ sin\,(33) = 30.07$$

$$Q_p = [9.19\, x\, L][30.07][\pi\, \frac{(0.4)^2}{4}] = 34\, L$$

Then total pile capacity Q_o (shaft + point) is:

$$Q_o = 34\, L + 5.68\, L^{1.55}$$

Using a factor of safety equal to 3.0, the allowable total pile capacity Q_{all}, is:

$$Q_{all} = \frac{Q_o}{FS} = \frac{34\, L + 5.68\, L^{1.55}}{3} = 1000$$

Solving this equation yields L = 39.13 m.

Considering pile set-up:

Total pile capacity at the end of initial driving, Q_o, is:

$$Q_o = 34\,L + 5.68\,L^{1.55}$$

Using equation (12-a,b) gives:

$$A = 0.005 \times \left(\frac{L}{0.4}\right) exp(0.6 \ \ tan\,(33^\circ)) = 0.018L$$

As stated earlier, most of set-up in cohesionless soils occurs within 15 days after the end of initial driving. As such total pile capacity 15 days after EOID is:

$$Q_t = Q_o[1 + 0.018 \times L \times \log(15 / 0.5)]$$

Using a factor of safety equal to 3.0, the allowable total pile capacity considering set-up is:

$$Q_{all} = \frac{Q_t}{FS} = \frac{Q_o[1 + 0.018\ x\ L\ x \log(15 / 0.5)]}{3} = 1000$$

Solving this equation yields L = 27.21 m.

This example indicates clearly that the percent of reduction in pile penetration depth when set-up is considered in design is 31%, and this definitely leads to considerable savings in the cost of pile driving as well as in the cost of pile material.

CONCLUSIONS

On the basis of the work performed in this study, the following conclusions are drawn:

1. Pile capacity in cohesionless soil increases with time, and this increase may continue up to a time longer that 200 days. The magnitude of the increase in pile capacity as indicated by the data base of this study is significant and may reach as high as 300% of the initial pile capacity after the end of initial driving.
2. The increase in pile capacity up to a time longer than 24 hours after pile driving together with the magnitude of the observed set-up indicate that dissipation of excess pore water pressure doesn't account for the observed increase in pile capacity with time and that other mechanisms contribute to the observed pile set-up in the field.
3. Pile set-up primarily results from the increase in pile shaft capacity with time.
4. The scatter in data which is obvious in the plots of set-up versus time is mainly due to the dependency of the magnitude of set-up on a combination of a number of influencing factors related to some extent to soil properties and pile characteristics.
5. The magnitude of the observed set-up is large for small diameter piles and decreases with increasing pile diameter. The magnitude of set-up increases with increasing pile penetration depth. It seems that pile slenderness ratio (*L/D*) is the most significant factor affecting the magnitude of set-up. Set-up increases with increasing (*L/D*) ratio.
6. Set-up is derived from shaft capacity rather than toe capacity. No significant increase in toe capacity with time is observed. The variation of shaft capacity with time shows the same trend of the total observed set-up with time.
7. Simplified empirical correlations are developed in this study to predict the magnitude of set-up. A design method for driven piles in cohesionless soils that accounts for set-up is also proposed in this study. The application of the proposed method to solve a hypothetical example indicates that significant savings in pile penetration depth and diameter and a reduction in size of driving equipment will be achieved by considering pile set-up in design.

REFERENCES

Alawneh, A.S., Nusier, O.K., Hussein Malkawi, A.I. and Al-Kateeb, M.I. 2001. Axial Compressive Capacity of Driven Piles in Sand: A Method Including Post-Driving Residual Stress, *Canadian Geotechnical Journal*, 38: 364-377.

Axelsson, G. 1998. Long-Term Set-Up of Driven Piles in Non-cohesive Soils Evaluated from Dynamic Tests on Penetration Rods, *Proceedings of the First International Conference on Site Characterization*, 2: 895-900.

Axelsson, G. 2000. Set-Up of Driven Piles in Sand-The Effect of Constrained Dilatancy During Loading, *Proceedings of the International Conference on Geotechnical and Geotechnical Engineering*, GeoEng 2000, Melbourne, Australia.

Axelsson, G. 2000. Long-Term Set-up of Driven Piles in Sand, Doctoral Thesis, Department of Civil and Environmental Engineering, Royal Institute of Technology, Stockholm.

Bogard, J. D. and Matlock, H. 1990. Application of Model Pile Test to Axial Pile Deign, *Proceedings of the 22nd Annual Offshore Technology Conference*, Texas, 3: 271-278.

Bowman, E.T. and Soga, K. 2005. Mechansims of Set-up of Displacement Pile in Sand: Laboratory Creep Test, *Canadian Geotechnical Journal*, 42: 1391-1407.

Bullock, P.J. and Schmertmann, J.H. 2003. Determination of the Effect of Stage Testing on the Dimensionless Pile Side Shear Setup Factor, *Final Report Contract #BC354 RPWO #27*, Prepared for University of Florida.

Castelli, R.J. and Hussein, M. 1998. Pile Foundation Construction for the Buckman Bridge, Jacksonville, Florida, *Proceedings of the 4th International Conference on Case Histories in Geotechnical Engineering*, Saint Louis, Missouri, Paper 11.01.

Chow, F.C., Jardine, R.J., Brucy, F. and Naroy, J.F. 1996. The Effect of Time on the Capacity of Pipe Piles in Sand, *Proceedings of the 28th Offshore Technology Conference*, Houston, Texas.

Chow, F.C., Jardine, R.J., Naroy, J.F. and Brucy, F. 1997. Time-Related Increases in the Capacities of Driven Piles in Sand, *Geotechnique*, 47 (2): 353-361.

Chow, F.C., Jardine R.J., Naroy, J.F. and Brucy, F. 1998. Effects of Time on Capacity of Pipe Piles in Dense Marine Sand, *Journal of Geotechnical Engineering, ASCE*, 124 (3): 254-264.

Fellenius, B.H. 1989. Prediction of Pile Capacity: Predicted and Observed Axial Behavior of Piles, *Geotechnical Special Publication No. 23, ASCE*, 293-302.

Fellenius, B.H., Riker, R.E., O'Brian, A.J. and Tracy, G.R. 1989. Dynamic and Static Testing in Soils Exhibiting Set-up, *Journal of Geotechnical Engineering, ASCE*, 115 (7): 984-1001.

Fellenius, B.H. and Altaee, A. 2002. Pile Dynamics in Geotechnical Practice – Six Case Histories, *Deep Foundations Congress, Geotechnical Special Publication* (116): 1, *ASCE*, Reston, Virginia.

Hussein, M.H., Sharp, M.R. and Knight, W.F. 2002. The Use of Superposition for Evaluating Pile Capacity, *Deep Foundations Congress, Geotechnical Special Publication* (116): 1, *ASCE, R*eston, Virginia.

Komurka, V.E. 2002. Incorporating Set-up into the Design and Installation of Driven Piles, *The 3rd Annual Design and Installation of Cost-Efficient Driven Piles Symposium*, PDCA, New Orleans, Louisiana.

Long, J.H., Kerrigan, J.A. and Wysockey, M.H. 1999. Measured Time Effects for Axial Capacity of Driven Piling, *Transportation Research Record* 1663, Paper (99): 1183, 8-15.

Plantema, G. 1948. The Occurrence of Hydrodynamic Stresses in the Pore Water of Sand Layers During Driving of Piles, *Proceedings of the 2nd International Conference in Soil Mechanics and Foundation Engineering*, Rotterdam, 4: 127-128.

Peck, R.B., Hanson, W.E. and Thournburn, T.H. 1973. Foundation Engineering, Wiley, 312.

Saxena, D.S. 2004. Case Histories of a Five –Story Printing Press Foundation with Zero Movement Criterion, *The 57th Canadian Geotechnical Conference*, Quebec City, Canada.

Schmertmann, J.H. 1991. The Mechanical Aging of Soils, 25th Terzaghi Lecture, *Journal of Geotechnical Engineering, ASCE*, 117: 1288-1330.

Sevilla, C.M., Gilroy, J.M. and Jenkins, J. 1998. Results of Dynamic Testing on Friction H Piles, Proceedings of the *4th International Conference on Case Histories in Geotechnical Engineering*, Saint Louis, Missouri, 3.06.

Skov, R. and Denver, H. 1988. Time-Dependence of Bearing Capacity of Piles, *Proceedings of the 3rd International Conference on Application of Stress-Waves to Piles*, 1-10.

Svinkin, M.R. 1996. Setup and Relaxation in Glacial Sand-Discussion, *Journal of Geotechnical Engineering*, 122 (4) *ASCE*, 319-321.

Svinkin, M.R. 2002. Engineering Judgement in Determination of Pile Capacity by Dynamic Methods, *Deep Foundations Congress, Geotechnical Special Publication* (116):2, *ASCE*, Reston, Virginia, 898-914.

Tan, S.L., Cuthbertson, J.K. and Robert, E. 2004. Prediction of Pile Set-up in non-Cohesive Soils, *Journal of Geotechnical Engineering*, 120 (1), *ASCE*, 50-65.

Tavenas, F. and Audy, R. 1972. Limitations of the Driving Formulas for Predicting Bearing Capacities of Piles in Sand, *Canadian Geotechnical Journal*, 9: 47-62.

York, D.L., Brusey, W.G., Clemente, F.M. and Law, S.K. 1994. Set-up and Relaxation in Glacial Sand, *Journal of Geotechnical Engineering*, 120 (9), *ASCE*, 1498-1513.